Supplementary material:
Non-invasive super-resolution imaging through dynamic scattering media

Dong Wang[1,2,#], Sujit K. Sahoo[1,3,#] Xiangwen Zhu[1],

Giorgio Adamo[4] and Cuong Dang[1,*]

[1] Centre for Optoelectronics and Biophotonics (COEB), School of Electrical and Electronic Engineering, The Photonics Institute (TPI), Nanyang Technological University Singapore, 50 Nanyang Avenue, 639798, Singapore

[2] Key Laboratory of Advanced Transducers and Intelligent Control System, Ministry of Education, and Shanxi Province, College of Physics and Optoelectronics, Taiyuan University of Technology, Taiyuan 030024, China

[3] School of Electrical Sciences, Indian Institute of Technology Goa, Goa 403401, India

[4] Centre for Disruptive Photonic Technologies, SPMS, TPI, Nanyang Technological University, Singapore 637371, Singapore

[#] Dong Wang and Sujit K. Sahoo contribute equally.

* Corresponding author, E-mail: HCDang@ntu.edu.sg

1. Optical experiment setup

The optical setup for experimental demonstration of stochastic optical scattering localization imaging (SOSLI) is depicted schematically in supplementary Fig. S1. It consists of two parts: the object simulator, and the imaging setup. The former is designed for convenient generation of various objects with blinking emitters. We replace the projection lens of a commercial projector (Acer X113PH) by a microscope objective (40x, numerical aperture: NA=0.65) to de-magnify the projector pixels to 1.34×1.34 μm^2 squares at the object plane. Two irises, one placed in front of the projector and the other at the object plane, are used to block all the stray light generated by the projector. Light from the object passing through both scattering media and the imaging iris, is captured by a camera sensor (Andor Neo 5.5, 2560×2160 pixels, and

6.5-µm pixel size). The scattering media are a ground glass diffuser (a static one) or a fresh chicken eggshell membrane (a dynamic one) in our demonstration. An optical filter (Thorlabs FB550-10, 550 nm wavelength, and 10 nm full-width at half-maximum - FWHM) is mounted on the camera to narrow the optical spectrum. Blinking emitters are generated by randomly blinking projector pixels. For invasive measurement of the point spread function (PSF), only one center pixel is turned on.

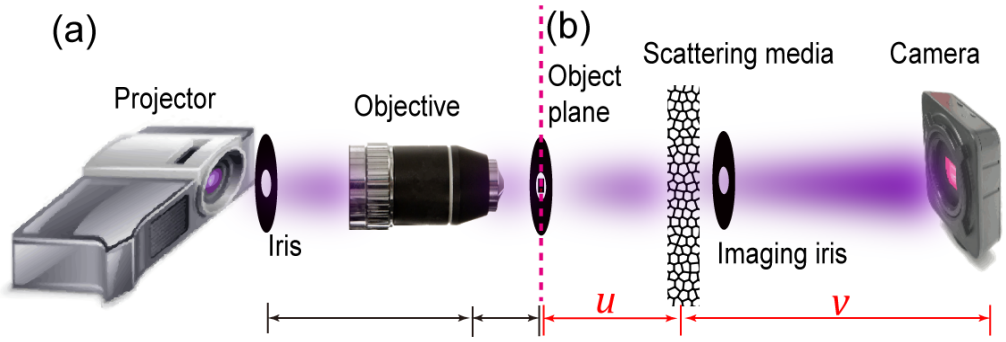

Supplementary Fig. S1. Optical setup to demonstrate SOSLI for non-invasive super-resolution imaging through strongly scattering media. (a) Object-simulator, which is designed for generating various microscopic objects at the object plane. **(b)** Simple optical configuration for imaging setup where u = 10 mm and v = 100 mm.

2. The current state-of-the-art non-invasive and invasive imaging

We conduct experiments for the demonstration of the current state-of-the-art non-invasive and invasive imaging through a 120-grit ground glass diffuser using the experimental setup shown in supplementary Fig. S1. A non-invasive image is retrieved from the autocorrelation of a single-shot speckle pattern by applying the phase retrieval algorithm. An invasive image is the deconvolution of a single-shot speckle pattern with an invasively measured PSF. The diameters of the imaging iris are set as 1 mm, 2 mm and 3 mm that correspond to NAs of 0.05, 0.1 and 0.15, respectively, and diffraction limits of 6.7 µm, 3.4 µm and 2.3 µm respectively. We can easily see the effects of NA on resolution from the results given in supplementary Fig. S2. An imaging system is a low pass filter, where higher NA (higher cut-off frequency) provides higher resolution (i.e. sharper) images than lower NA does. Because of the effects of noise, camera's dynamic range and dark counts on the performance of the phase retrieval algorithm, the single-shot non-invasive images have a slightly lower resolution than the diffraction limit. If these effects are too high, the algorithm may not even converge. On the other hand, the deconvolution images have a slightly higher resolution than the diffraction limit because deconvolution recovers and enhances the high frequency components of images, i.e. sharper cut-off low pass filter.

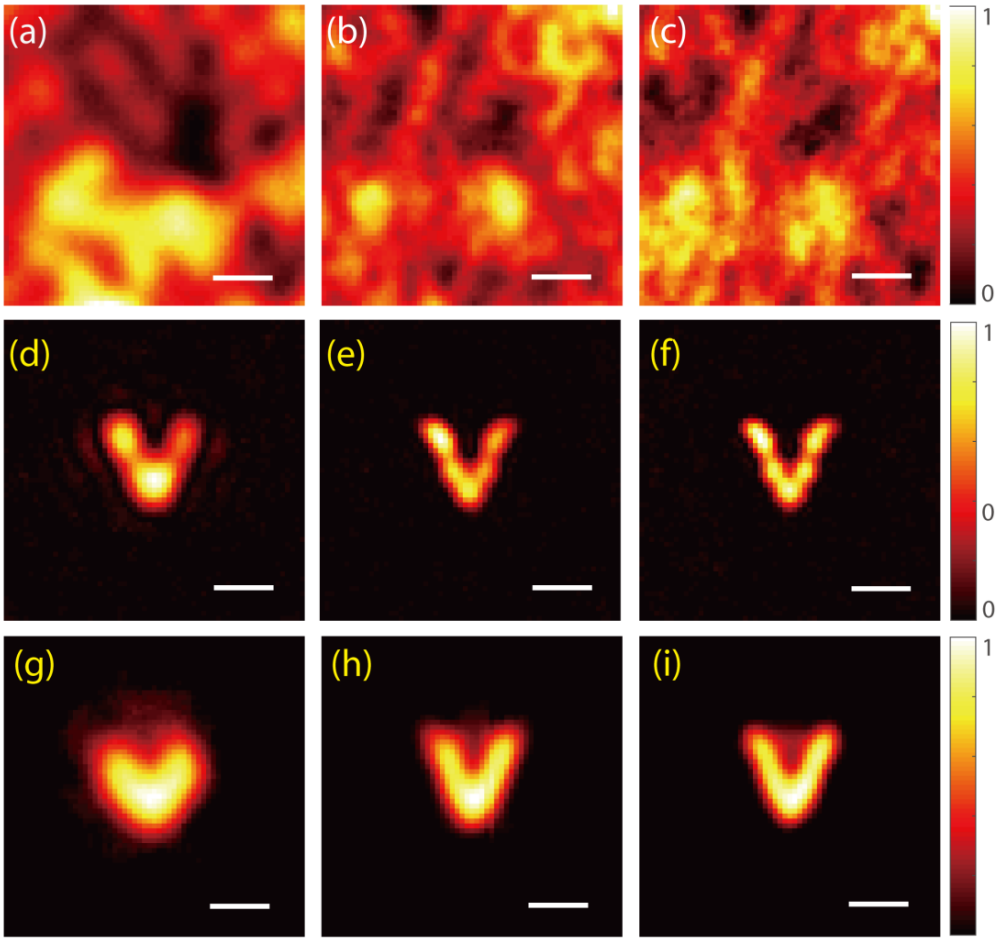

Supplementary Fig. S2. The effect of NA on resolution for invasive and non-invasive imaging through scattering media. (a-c) The speckle patterns of the same object with NAs of 0.05, 0.1, and 0.15, respectively. Experimental results of the state-of-the-art invasive **(d-f)** and non-invasive **(g-i)** imaging through the 120-grit ground glass diffuser with the speckle patterns in (a-c) respectively. Scale bar: 10 camera pixels, equivalent to 6.5 μm on the object plane.

3. Multiple estimated PSFs from a single stochastic speckle pattern

From a series of stochastic speckle patterns recorded for SOSLI, we pick up one pattern randomly (Fig. S3a). The iterative phase retrieval algorithm is utilized to retrieve the emitter pattern at low resolution as presented in Fig. S3b-c. Two similar emitter patterns shifted from each other can be retrieved from a single speckle pattern by two different runs of the algorithm because autocorrelation only keeps the relative emitter positions while losing their exact positions. Figure S3d-e present the emitter positions after localization. The localized-emitter images show very clean emitters, removing all the noise or artifacts of the phase retrieval algorithm. Figure S3f-g show the estimated PSFs calculated from a single speckle pattern (Fig. S3a) and two different phase retrieval/localization results (Fig. S3d-e). Figure S3i-j present the emitter positions localized after deconvolution of another speckle pattern (Fig. S3h) with two estimated

PSFs in Fig. S3f-g. The emitter positions in Fig. S3i-j automatically align very well with those in Fig. S3d-e, respectively because they are reconstructed from the same estimated PSFs. The absolute positions of emitters and PSF are not important in our SOSLI. They do not affect our results and usual imaging techniques do not concern about absolute position.

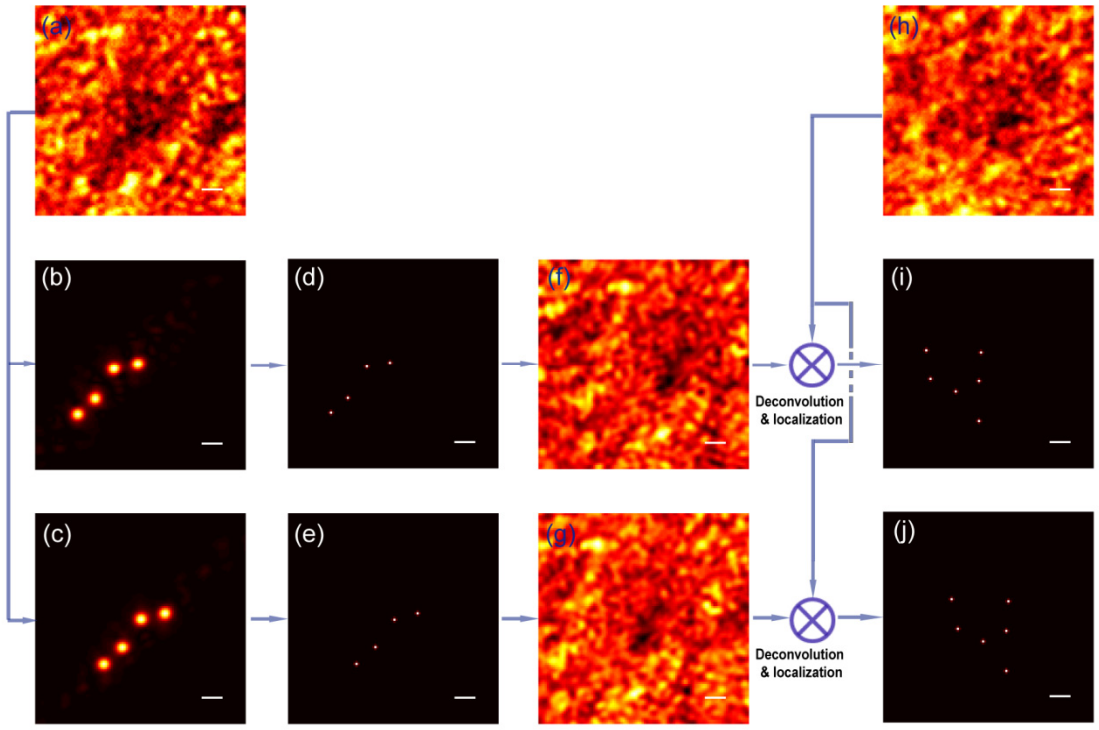

Supplementary Fig. S3. Deconvolution process with different estimated PSF. (a) A typical stochastic speckle pattern. **(b-c)** Typical images retrieved from autocorrelation by phase retrieval algorithm. **(d-e)** Localized-emitter images. **(f-g)** Estimated PSFs. **(h)** Another stochastic speckle pattern. **(i-k)** Emitter positions calculated from a single speckle pattern and two estimated PSFs. Scale bar: 10 camera pixels, equivalent to 6.5 μm on the object plane.

4. SOSLI with PSFs estimated from different speckle patterns

During our implementation of SOSLI, we randomly choose one pattern out of multiple collected speckle patterns for estimation of the PSF. Interestingly, different speckle patterns give us slightly different estimated PSFs. The differences are not only arbitrary shift from each other but also the speckles themselves (supplementary Fig. S4a-f and S5b-c). However, the reconstructed images from these estimated PSFs are very much similar (supplementary Fig. S4g-i) with different shifts. It implies that we only estimate the main features of the PSF, which is sufficient for reconstruction. We test the similarity of these three estimated PSFs by calculating the correlation among them. The autocorrelation of PSF1 shows its random speckle nature with a bright spot (Gaussian

profile) at the center (supplementary Fig. S5a). The correlation of PSF1 with the other PSFs indicates an off-center bright spot with some background (supplementary Fig. S5b-c), implying that these PSFs share the main features and shift from each other. The clear bright spot allows us to locate its center then obtain the relative shift between PSFs. The obtained relative shifts (supplementary Fig. S5d) are exactly equal to the relative shifts between the retrieved objects (supplementary Fig. S4g-i).

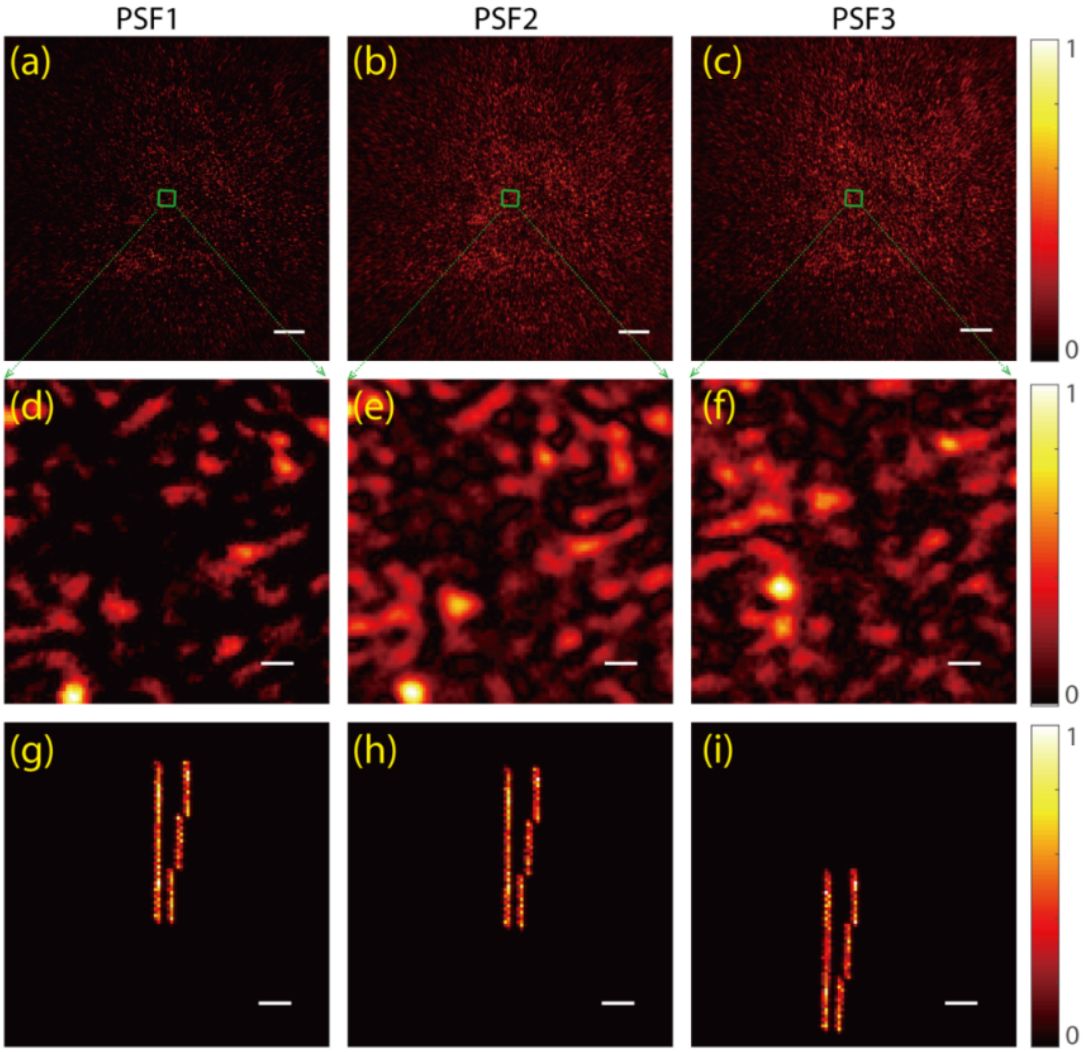

Supplementary Fig. S4. Retrieved results of an object with the PSFs estimated from different speckle patterns arbitrarily chosen. (a-c) The estimated PSFs (full scale), **(d-f)** The zoomed-in center part of corresponding PSFs in a-c. **(g-i)** The corresponding super-resolution SOSLI results. Scale bar: 200 camera pixels for a-c, and 10 camera pixels for d-i, which is equivalent to 6.5 μm on the object plane.

The observation is interesting, important and useful. Because of the localization, we can easily remove the background artifact and noise in the phase retrieval images and deconvolution images. Therefore, the SOSLI approach can tolerate more error in PSF estimation. This not only explains how and why the SOSLI should work very well in

static scattering media, but also inspires us to conceive a successful solution for dynamic scattering media in section 7.

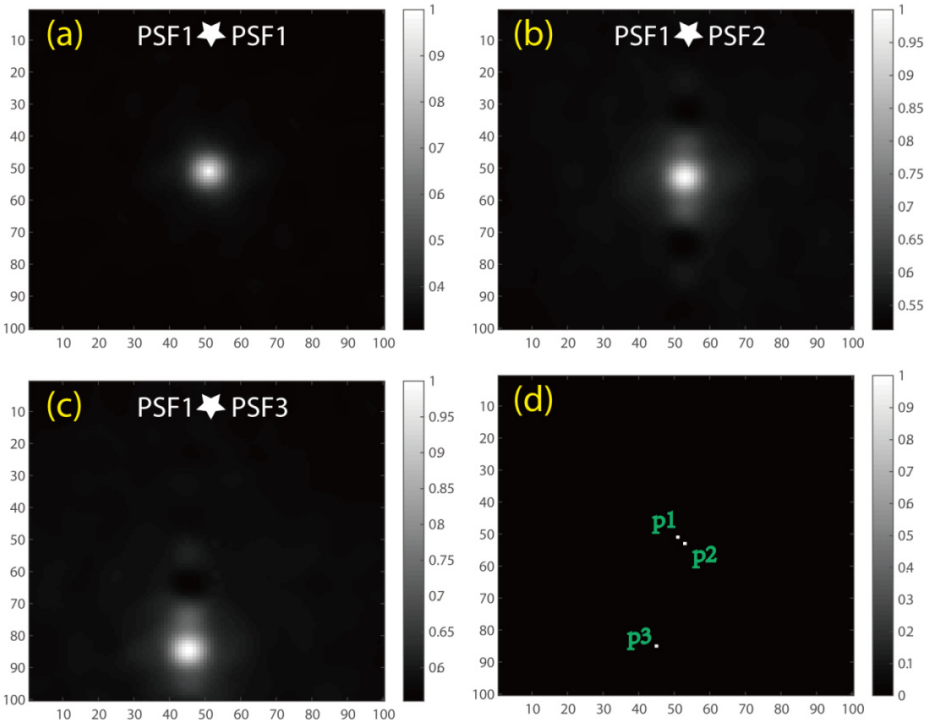

Supplementary Fig. S5. Cross-correlations of the PSF1 with the other PSFs to obtain the relative shifts between them. (a-c) The correlation patterns. **(d)** The relative shifts between PSF1 with other PSFs. The numbers on the side of image indicates the pixel numbers.

5. SOSLI with different numbers of stochastic patterns.

In our experiment, the object to be imaged through a diffuser constitutes multiple blinking emitters. The SOSLI technique reconstructs a super-resolution image from multiple stochastic patterns. The quality of the reconstructed image will increase with the number of frames. We characterize the reconstructed images with various numbers (n=200, 400, 800, and 8000) of the randomly blinking emitter patterns which are used Fig. 3c. The results are shown in supplementary Fig. S6 where supplementary Fig. S6e-h show the results of supplementary Fig. S6a-d after the bicubic interpolation processing. It is obvious that reconstruction with 8000 stochastic patterns gives the best image quality (supplementary Fig. S6d&h). However, 300-400 frames are sufficient for the reconstruction of our simple object (supplementary Fig. S6b&f).

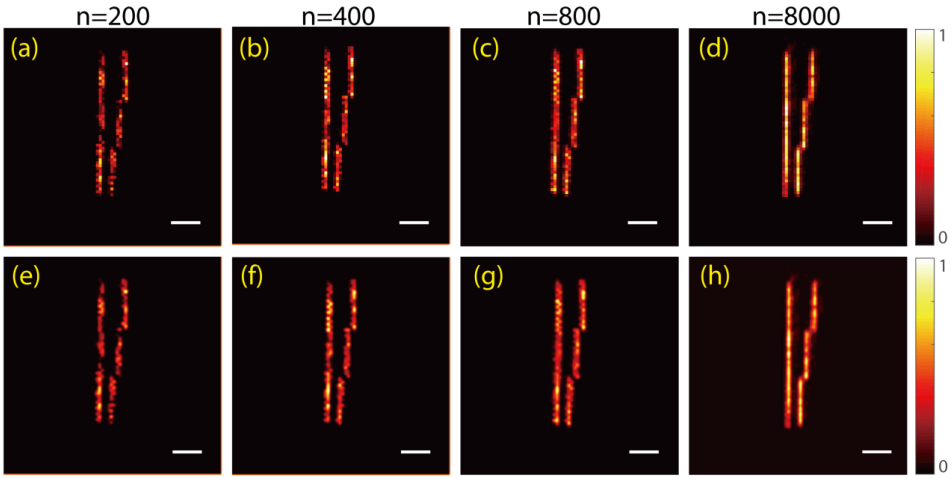

Supplementary Fig. S6. Retrieved results of an object by SOSLI with the different numbers of stochastic patterns. **(a-d)** The raw results from SOSLI. **(e-h)** The results after bicubic interpolation processing. Scale bars: 6.5 μm.

6. Deconvolution results with a decorrelated PSF

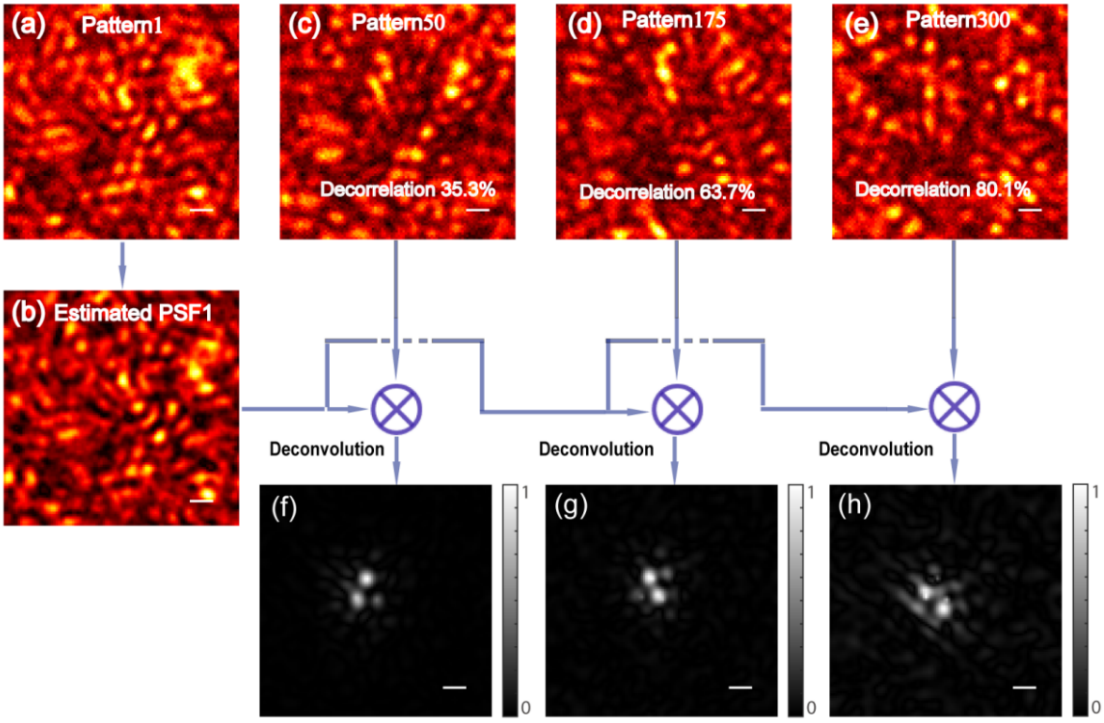

Supplementary Fig. S7. Deconvolution results with a decorrelated PSF of the chicken eggshell membrane. a) The first stochastic speckle pattern is chosen to estimate the PSF. **b)** The estimated PSF from the first stochastic speckle pattern (PSF1). **c-e)** The stochastic speckle patterns with the membrane's decorrelation (the correlation coefficients with respect to the pattern number are presented in Fig. 5a: 0.65, 0.36, 0.2 respectively). **f-h)** The deconvolution results of the speckle patterns in c-e, respectively, with the estimated PSF1 from the first speckle pattern. There are increasing artifacts in deconvolution images with increase of scattering media's decorrelation. Scale bar: 10 camera pixels, equivalent to 6.5 μm on the object plane.

7. PSF alignment for highly dynamic scattering media

The most adaptive SOSLI approach utilizes phase retrieval algorithm to correct the deconvolution image (with the PSF estimated from previous speckle pattern) while the deconvolution image is used to maintain no-shifting and no-flipping between two retrieved images for superposition. An additional step that check the shifting and flipping condition of the estimated PSF with the previous one could allow us to reconstruct super resolution images more reliably, enhancing resolution.

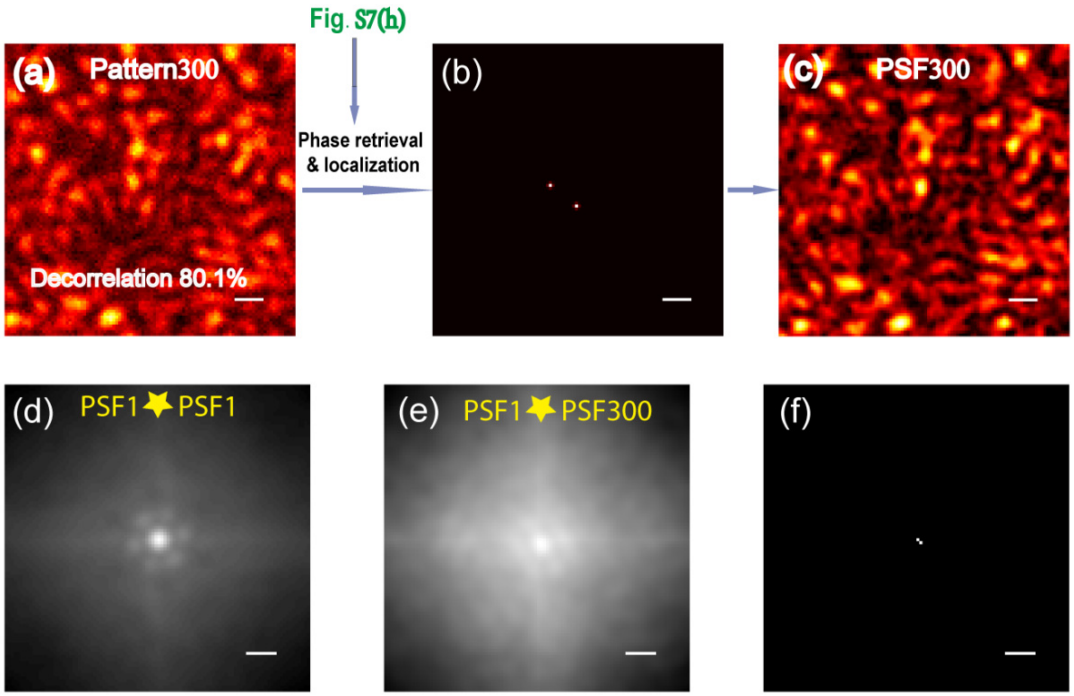

Supplementary Fig. S8. The most adaptive approach for SOSLI to mitigate highly dynamic scattering media. a) A speckle pattern (pattern 300) taken when scattering media decorrelate 80%, i.e. the correlation of 20%. **b)** An emitter pattern recovered from the speckle pattern in (a) by the phase retrieval algorithm with initial guess from Fig. S7(h) then localization. **c)** The estimated PSF from the speckle pattern in (a) and the emitter pattern in (b). **d)** The autocorrelation of PSF1, which is Fig. S6(b). **e)** The correlation between PSF1 and PSF300 (in figure c). **f)** The centers of brightest spots in d&e, showing the relative shift between two PSFs, which is also the relative shift between two emitter patterns derived from speckle pattern #1 and #300 by phase retrieval and localization. Scale bar: 10 camera pixels, equivalent to 6.5 μm on the object plane.

Here, we take 2 speckle patterns #1 and #300 as an example for 2 consecutive shots of highly dynamic scattering media, where the decorrelation is about 80%. Supplementary Fig. S7h presents the deconvolution image of speckle pattern 300 with the PSF1, which is estimated from speckle pattern 1. We use Fig. S7h as the initial

guess in phase retrieval algorithm for speckle pattern 300 (Fig. S8a) to achieve high quality image. Then, localization process provides precise emitter positions (Fig. S8b) with respect to those from pattern 1 for superposing in SOSLI. In some rare cases, noise and large decorrelation of scattering media in these two shots might cause some errors in relative positions between two reconstructed emitter patterns, degrading the resolution of SOSLI. To confirm and realign the relative position of reconstructed emitter patterns, we re-estimate the new PSF as PSF300 (Fig. S8c), then calculate the correlation of PSF1 with PSF300 as presented in Fig. S8e which has a bright spot on a strong background. The center of bright spot can be identified by localization algorithm. The offset of this correlation center from the image center (Fig. S8f) is the relative shift between two PSFs, which is also the relative shift between two reconstructed emitter patterns. If we fine tune the correction rate in phase retrieval algorithm carefully, we can achieve no offset most of the time, i.e. the cross-correlation pattern between PSF1 and PSF300 is similar to autocorrelation of PSF1 (Fig. S8d) with, certainly, a lot more background noise. However, such fine-tuning the parameters in phase retrieval algorithm depends on context and nature of the images. Therefore, we should always calculate the relative shift between 2 phase retrieved images, then realigning them before superposing to achieve better SOSLI results.

8. SOSLI with low-photon emitters

SOSLI relies on speckle patterns which are formed by photons from emitters. For each pixel in a speckle pattern, the intensity represents the probability that photons land at that pixel (Fig. S9a). If the number of photons is not enough, the speckle pattern is "underdeveloped", i.e. there is uncertainty in the captured speckle patterns (Fig. S9b-c). The first step in SOSLI is to perform a low-resolution image recovery for any pattern of the blinking emitters using phase retrieval algorithm and localization. Therefore, the success of SOSLI relies on the success of this first step. Hybrid-Input-Output (HIO) Fienup algorithm is used in our phase retrieval step, which is widely used for its simplicity and speed. However, its success varies, depending on the initial guess. Therefore, the usual practice is to run the algorithm with a few random starting guesses and choose a good result. In general, this algorithm converges for fully developed speckle patterns with almost any initial guess. An underdeveloped speckle pattern due to the low photon budget would corrupt the signal, thus, pose a big challenge for this step. Here, we perform a simulation to check the success rate at various photon budget as detailed below.

A typical noise-free speckle pattern is used as the "fully-developed" speckle pattern (Fig. S9a). The speckle patterns are then quantized to 32-bit numerical precision, which can be treated as a 2^{32}-photon counting capacity of each pixel. Taking this fully

developed quantized speckle pattern as the discrete photon distribution model (i.e. the probability mass function), samples of scattering photons are generated by Monte Carlo simulation. The image size is taken as 1024x1024 pixels, the photon budget is quantified as average photon per pixel (PPP). So total number of photons used for various speckle patterns is $PPP \times 1024 \times 1024$, which is distributed on 1024x1024 pixels according to the probability. Figure S9b-c show two typical speckle patterns with PPP = 0.7. The uncertainty of the speckle pattern can be easily observed. For our simulation, a total 60 random realizations are obtained for each PPP scenario; and for each realization of the speckle pattern, the phase retrieval algorithm is deployed with 60 random starting guesses. There are 3600 trials for each PPP.

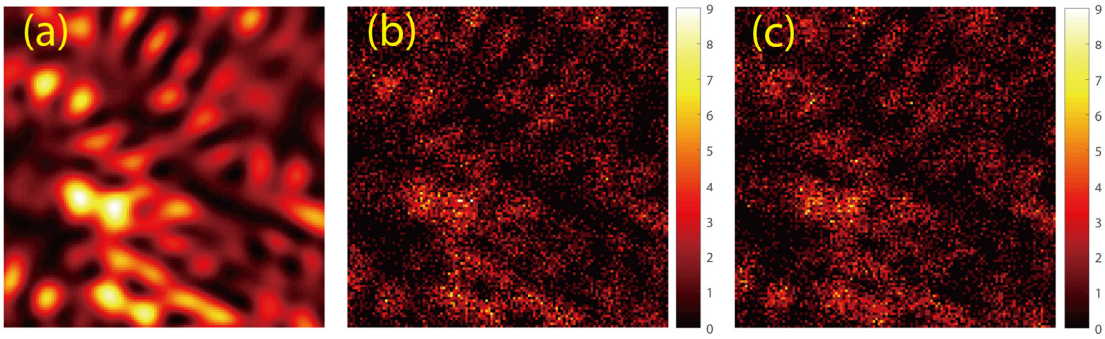

Supplementary Fig. S9: (a) A zoomed-in portion (128x128 pixel) of fully developed speckle pattern from one stochastic emitter pattern. **(b-c)** typical "underdeveloped" speckle patterns with the same PPP = 0.7.

The success rate is decided from the successful recovery of the object out of these 3600 trials. Here, a successful recovery is defined as the exact relative positions of the blinking emitters after the phase retrieval and localization. The sparsity of the object also helps phase retrieval algorithm to converge better. We choose the sparsest emitter pattern that has only 2 emitters to examine the lowest photon budget requirement. For an accurate classification of success, we compare the vector connecting two ground-truth emitters with the vector connecting two localized emitters (as well as its central flipping versions). The matching of vectors at single pixel level implies the success of this step without worrying about absolute position. Figure S10a-c describe one successful instance corresponding to PPP = 1, the phase-retrieved image (Fig. S10a) is good enough to localize emitters correctly (Fig. S10b) compared to the ground truth (Fig. S10c). Figure S10d plots the success rate as a function of PPP. With 1 photon per pixel, our chance of success in phase retrieval and localization is about 11%. This probability drops to 2.8% with PPP = 0.8.

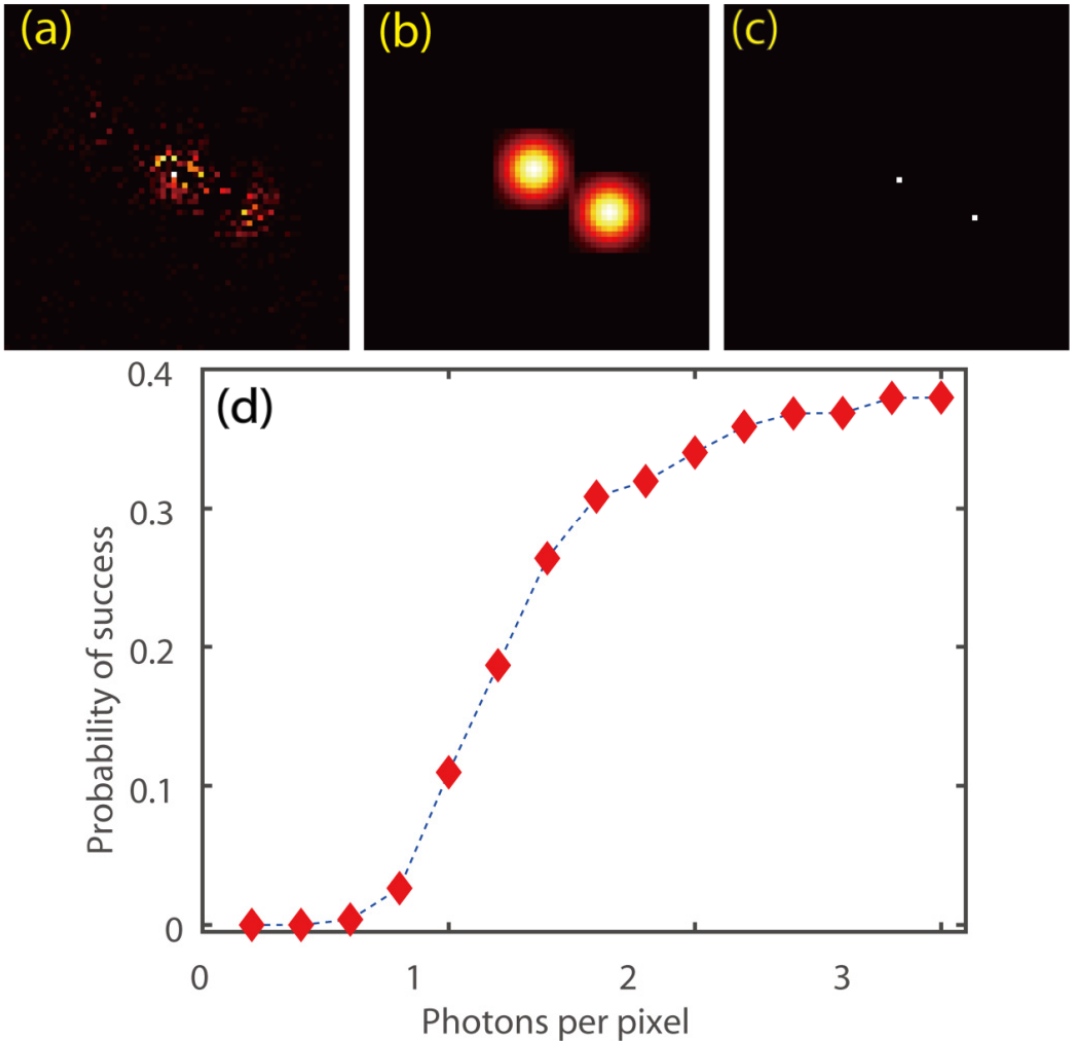

Supplementary Fig. S10: (a) A recovered object from a speckle pattern (PPP = 1.0) using phase retrieval. **(b)** Localization algorithm successfully finds 2 emitters from (a) using a 5x5 gaussian window, then the centers of these gaussian hot spots are identified. **(c)** The actual object. **(d)** Success rate of phase retrieval and localization is stated as probability of success in a trial for various photons per pixel scenario.

After a successful recovery of one stochastic object using phase retrieval algorithm and localization, the next step is to estimate the PSF using the recovered object and the low photon count image. Then the estimated PSF is used to recover the remaining stochastic emitters from their low photon count speckle patterns. Therefore, in the next simulation we will evaluate the success rate in recovering a different stochastic emitter pattern from the successful estimated PSF. Since the estimated PSF is going to be different for different random realizations of the speckle image, we take 60 estimated PSFs from previous successful step at each PPP. Using each estimated PSF, a different stochastic emitter pattern is recovered by deconvolution followed by localization from 60 random

realizations. Overall, we have 3600 trials to examine the success rate of deconvolution and localization process. Figure S11a-c show one example of estimated PSF with PPP = 0.7, the deconvolution image, and the localized emitters, respectively. Figure S11d plots the success rate evaluation at various PPP values. It shows that the deconvolution process is robust to low photon count in the evaluated range. It is also understandable that phase-retrieval is the bottleneck of SOSLI; if the signal is good enough for phase retrieval algorithm, the deconvolution will be successful.

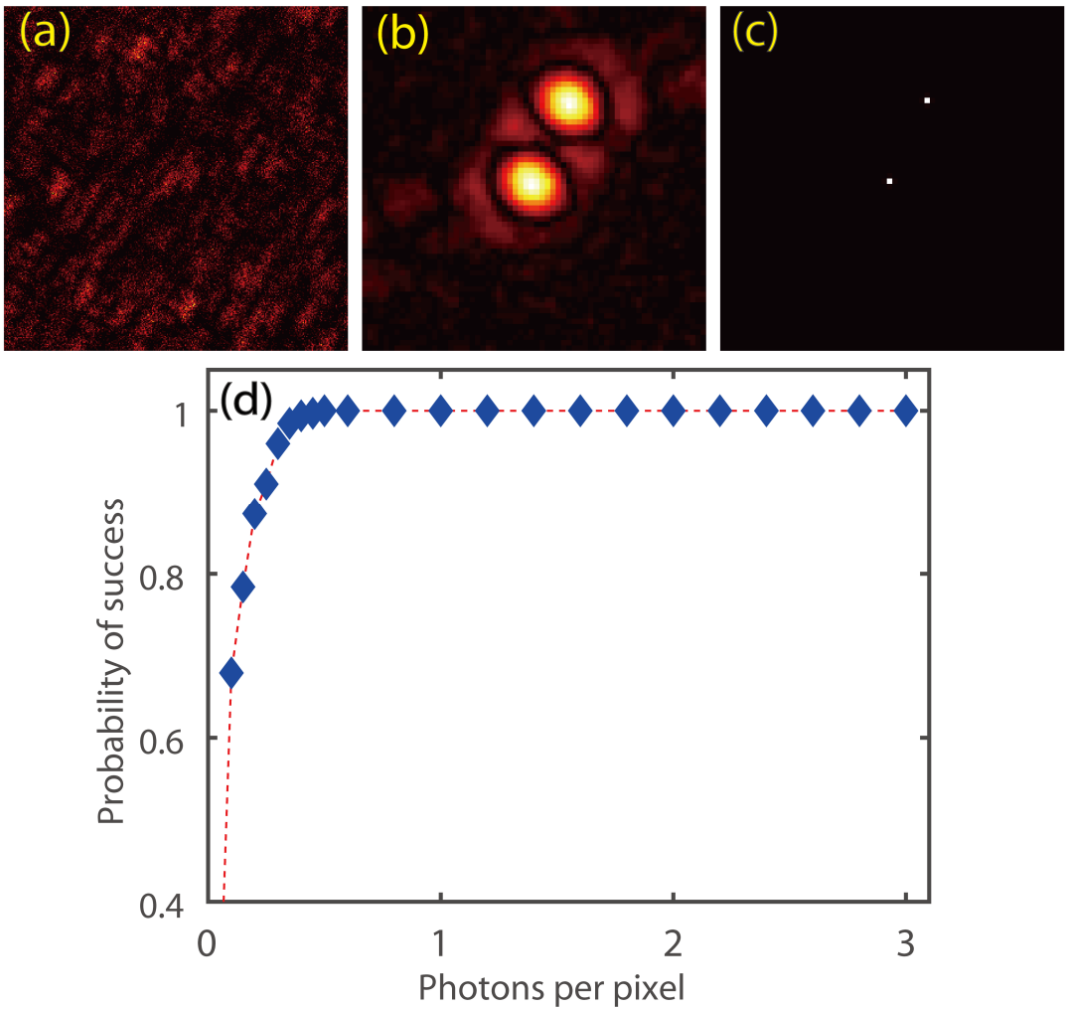

Supplementary Fig. S11: (a) An estimated PSF using the successful estimated object from the phase retrieval step. **(b)** A reconstructed stochastic object by deconvolution using the estimated PSF. **(c)** A super-resolution image after localization. **(d)** Success rate of deconvolution and localization is stated as the probability of success in a trial for various photons per pixel scenario.